QUATERNION GENERALIZED ORTHOGONAL MATCHING PURSUIT

FENG-JIE HE[1], CUI-MING ZOU[1]

[1]College of Informatics, Huazhong Agricultural University, Wuhan 430070, China
E-MAIL: hefengjie@webmail.hzau.edu.cn, zoucuiming2006@163.com

Abstract:

Quaternion Orthogonal Matching Pursuit (QOMP) pioneers the application of quaternions in color image processing, garnering widespread attention for its superior performance. However, it selects only one atom that is more correlated with the residual at each iteration, leading to a higher number of iterations. In particular, the atoms selected separately by QOMP at each step may not always come from the same subspace, which can potentially reduce the algorithm's accuracy. This paper proposes a Quaternion Generalized Orthogonal Matching Pursuit (QGOMP) model that can select multiple atoms each time. Specifically, it optimizes the atoms selection strategy by leveraging the correlation between atoms within the same subspace, which significantly reduces the number of iterations while enhancing the accuracy of sparse signal recovery. The experimental results reveal the competence of QGOMP in various color image recognition and clustering using standard datasets.

Keywords:

Quaternion orthogonal matching pursuit; quaternion sparse representation; color image.

1 Introduction

Orthogonal Matching Pursuit (OMP) [1] is a widely used greedy algorithm for sparse representation. It iteratively selects the most correlated atoms to the residual and updates the residual via orthogonal projection, which efficiently constructs a sparse representation to recover the signals with single channel. However, for multichannel signals (such as color images and hyperspectral data), OMP can only process each channel separately, which fails to employ the correlation information between different channels.

In recent years, the widespread applications of multichannel signals have spurred significant research interest. For example, tensor or quaternion representation methods have rapidly developed to address this limitation. In particular, quaternion can integrate red, green, blue channels information for color images into a quaternion structure, which have shown to be effectively preserved intrinsic correlations between channels [2]. Xu et al. proposed a Quaternion Orthogonal Matching Pursuit (QOMP) model [3] for color image processing. However, it may face the issue of selecting atoms from different classes in the dictionary during each iteration when the signal has structural priors. To address this limitation, Dong et al. proposed a robust Quaternion Block Orthogonal Matching Pursuit (RQBOMP) [4] algorithm, which fully utilized the block structure information in the data to improve the performance of representing the data.

In fact, numerous studies remain committed to enhancing the performance of OMP for single-channel sparse signal recovery by focusing on how to select atoms more efficiently during iterations. For example, the Regularized Orthogonal Matching Pursuit (ROMP) method [5] introduced a regularization mechanism to ensure that the atoms selected in each iteration have a high level of confidence. The Generalized Orthogonal Matching Pursuit (GOMP) method [6] selected the most relevant multiple indices in each iteration, reducing the number of iterations. The GOMP method achieved efficient sparse signal recovery while also exhibiting adaptability to different task requirements. Currently, studies on the GOMP model in the quaternion setting have not been fully explored.

This paper is outlined as follows. Section 2 briefly introduces the basic facts for quaternion and some related works. Section 3 proposes a Quaternion Generalized Orthogonal Matching Pursuit (QGOMP) model and its algorithm for sparse signal representation, which is applied to quaternion sparse signal recovery, classification, and clustering tasks. Section 4 presents the experimental results for color face recovery, recognition, and clustering.

Section 5 concludes this paper.

2 Related works

This section offers a review of the fundamental concepts of quaternions and the QOMP algorithm.

2.1 Quaternion

The quaternion $\dot{q} \in \mathbb{H}$, as a hypercomplex number, was invented by Hamilton [7]. It is constructed linearly by one real part and three imaginary parts, i.e., $\dot{q} = q_0 + q_1\mathrm{i} + \mathrm{q}_2\mathrm{j} + \mathrm{q}_3\mathrm{k}$, with $q_i \in \mathbb{R}$, $(i = 0, 1, 2, 3)$. The three imaginary parts obey these multiplication rules $\mathrm{ij} = -\mathrm{ji} = \mathrm{k}, \mathrm{jk} = -\mathrm{kj} = \mathrm{i}, \mathrm{ki} = -\mathrm{ik} = \mathrm{j}$, which indicates the quaternion multiplication is non-commutative. The conjugation of $\dot{q}$ is $\overline{\dot{q}} = q_0 - q_1\mathrm{i} - \mathrm{q}_2\mathrm{j} - \mathrm{q}_3\mathrm{k}$ and its modulus is $|\dot{q}| = \sqrt{\overline{\dot{q}}\dot{q}}$. A quaternion vector $\dot{\mathbf{x}} = (\dot{x}_1, \dot{x}_2, \ldots, \dot{x}_m)^T \in \mathbb{H}^m$ can be expressed as $\dot{\mathbf{x}} = \mathbf{x}_0 + \mathbf{x}_1\mathrm{i} + \mathbf{x}_2\mathrm{j} + \mathbf{x}_3\mathrm{k}$, where $\mathbf{x}_i \in \mathbb{R}^m$ $(i = 0, 1, 2, 3)$ are real-valued vectors. The conjugate transpose of $\dot{\mathbf{x}}$ is defined as $\dot{\mathbf{x}}^H = \left[\overline{\dot{x}_1}, \overline{\dot{x}}_2, \ldots, \overline{\dot{x}}_m\right]$, and the left inner product of two vectors is $\langle \dot{\mathbf{x}}, \dot{\mathbf{v}} \rangle := \dot{\mathbf{x}}^H \dot{\mathbf{v}}$. The ℓ_0 norm $\|\dot{\mathbf{x}}\|_0$ is the count of non-zero quaternions in $\dot{\mathbf{x}}$. The ℓ_2 norm of $\dot{\mathbf{x}}$ is calculated as $\|\dot{\mathbf{x}}\|_2 = \sqrt{\dot{\mathbf{x}}^H \dot{\mathbf{x}}} = \left(\sum_{i=1}^{m} |\dot{x}_i|^2\right)^{\frac{1}{2}}$.

2.2 Quaternion orthogonal matching pursuit

Sparse signal recovery aims to reconstruct a S sparse signal (with S non-zero elements) from limited linear measurements. QOMP is a crucial greedy algorithm for multi-channel signal processing[8]. Concretely, to obtain a S sparse vector $\dot{\mathbf{x}} \in \mathbb{H}^n$ for a test sample $\dot{\mathbf{y}} \in \mathbb{H}^m$ using a quaternion dictionary matrix $\dot{\mathbf{D}} = \left[\dot{\mathbf{d}}_1, \dot{\mathbf{d}}_2, \ldots, \dot{\mathbf{d}}_n\right] \in \mathbb{H}^{m \times n}$, where $\dot{\mathbf{d}}_i$ are atoms from samples, the QOMP model is the minimization problem as follows

$$\dot{\mathbf{x}}^* = \arg\min_{\dot{\mathbf{x}} \in \mathbb{H}^n} \left\|\dot{\mathbf{y}} - \dot{\mathbf{D}}\dot{\mathbf{x}}\right\|_2^2, \quad \text{s.t.} \quad \|\dot{\mathbf{x}}\|_0 \leq \mathrm{S}. \tag{1}$$

The QOMP selects the most correlated dictionary atom to the current residual in each iteration until a predefined sparsity threshold $\|\dot{\mathbf{x}}\|_0 \leq S$ is satisfied, effectively addressing the NP-hard ℓ_0 problem. On the basis of preserving the fundamental performance of QOMP, it is still possible to further reduce the algorithmic complexity and accelerate the running time. For example, Wang et al. propose an improved Generalized Orthogonal Matching Pursuit (GOMP) algorithm in single-channel sparse signal recovery [9]. In each iteration, GOMP selects multiple correlated atoms and adds several correct indices into the index set. GOMP enhances the efficiency of sparse signal reconstruction while maintaining high precision, and it requires significantly fewer iterations than OMP.

3 Method

This section proposes a Generalized Orthogonal Matching Pursuit (QGOMP) model and applies the QGOMP algorithm to signal recovery, recognition and clustering.

3.1 Quaternion generalized OMP

To further accelerate QOMP, we propose an improved algorithm that selects multiple most relevant atoms per iteration for multi-channel signals. Specifically, define a N-class dictionary $\dot{\mathbf{D}} = [\dot{\mathbf{D}}_{C_1}, \ldots, \dot{\mathbf{D}}_{C_N}] \in \mathbb{H}^{m \times n}$, where $\dot{\mathbf{D}}_{C_i}$ $(i = 1, 2, \cdots, N)$ are the sub-matrix of class i and $C_1 \cup C_2 \cup \cdots \cup C_N = C$ is the index set of all training samples. $\dot{\mathbf{D}}_\Lambda$ is a sub-matrix of $\dot{\mathbf{D}}$ with columns indexed by set Λ, where $\Lambda \subseteq C$. To improve QOMP by identifying the most relevant $s_0 \geq 1$ atoms in one iteration, we propose a Quaternion Generalized Orthogonal Matching Pursuit algorithm (QGOMP). When $s_0 = 1$, QGOMP returns to QOMP. The QGOMP algorithm is detailed as follows.

1) Initialization: we initialize the number of iterations $k = 0$, residual $\dot{\mathbf{r}}^{(0)} = \dot{\mathbf{y}}$ and index set $\Lambda^{(0)} = \emptyset$.

2) s_0-Identification: In the k-th iteration, QGOMP selects the top s_0 (integer $s_0 \geq 1$) atoms with the largest projections onto the current residual. Specifically, define the index set $I^{(k)} = \{I_1^{(k)}, \ldots, I_{s_0}^{(k)}\}$, where

$$I_i^{(k)} = \mathrm{argmax}_{i \in C \setminus \left(\Lambda^{(k-1)} \cup \left\{I_{s_0-1}^{(k)}, \ldots, I_1^{(k)}\right\}\right)} \left|\left\langle \dot{\mathbf{d}}_i, \dot{\mathbf{r}}^{(k-1)} \right\rangle\right|, \tag{2}$$

i.e., obtain indices based on the top s_0 correlations between atoms in the candidate pool $\dot{\mathbf{D}} \backslash \dot{\mathbf{D}}_{\Lambda^{(k-1)}}$ and the current residual, where $\dot{\mathbf{D}} \backslash \dot{\mathbf{D}}_{\Lambda^{(k-1)}}$ is a sub-matrix of $\dot{\mathbf{D}}$ excluding the columns indexed by $\Lambda^{(k-1)}$. Subsequently, we update the most relevant index set $\Lambda^{(k)} = \Lambda^{(k-1)} \cup I^{(k)}$.

3) Representation: Then update the representation subvector $\dot{\mathbf{x}}_{\Lambda^{(k)}}^{(k)}$ whose the atoms supported in $\Lambda^{(k)}$ by solving

$$\dot{\mathbf{x}}_{\Lambda^{(k)}}^{(k)} = \arg\min_{\dot{\mathbf{x}}_{\Lambda^{(k)}} \in \mathbb{H}^{\left|\Lambda^{(k)}\right|}} \frac{1}{2} \left\|\dot{\mathbf{y}} - \dot{\mathbf{D}}_{\Lambda^{(k)}} \dot{\mathbf{x}}_{\Lambda^{(k)}}\right\|_2^2, \tag{3}$$

the elements of $\dot{\mathbf{x}}^{(k)}$ that are not supported by $\Lambda^{(k)}$ are zeros, and sub-matrix $\dot{\mathbf{D}}_{\Lambda^{(k)}} \in \mathbb{H}^{m\times|\Lambda^{(i)}|}$. The non-commutativity of quaternion multiplication makes traditional real-valued gradient methods inapplicable to quaternion models, increasing the difficulty of solving problem (3). Inspired by auxiliary operators $\mathcal{P}$, $\mathcal{Q}$ and $\mathcal{Q}^{-1}$ (the inverse of $\mathcal{Q}$)[10], we establish an equivalent model of Eq. (3) as

$$\dot{\mathbf{x}}^{(k)}_{\Lambda^{(k)}} = \underset{\dot{\mathbf{x}}_{\Lambda^{(k)}}\in\mathbb{H}^{|\Lambda^{(k)}|}}{\arg\min} \frac{1}{2}\left\|\mathcal{Q}(\dot{\mathbf{y}}) - \mathcal{P}\left(\dot{\mathbf{D}}_{\Lambda^{(i)}}\right)\mathcal{Q}(\dot{\mathbf{x}}_{\Lambda^{(k)}})\right\|_2^2, \tag{4}$$

where $\mathcal{Q}(\dot{\mathbf{y}}) := \begin{bmatrix}\mathbf{y}_0^T & \mathbf{y}_1^T & \mathbf{y}_2^T & \mathbf{y}_3^T\end{bmatrix}^T \in \mathbb{R}^{4m}$, $\mathcal{Q}(\dot{\mathbf{x}}_{\Lambda^{(k)}}) \in \mathbb{R}^{4|\Lambda^{(k)}|}$,

$$\mathcal{P}(\dot{\mathbf{D}}) := \begin{bmatrix}\mathbf{D}_0 & -\mathbf{D}_1 & -\mathbf{D}_2 & -\mathbf{D}_3\\ \mathbf{D}_1 & \mathbf{D}_0 & -\mathbf{D}_3 & \mathbf{D}_2\\ \mathbf{D}_2 & \mathbf{D}_3 & \mathbf{D}_0 & -\mathbf{D}_1\\ \mathbf{D}_3 & -\mathbf{D}_2 & \mathbf{D}_1 & \mathbf{D}_0\end{bmatrix} \in \mathbb{R}^{4m\times 4n}. \tag{5}$$

Setting the derivative of $\mathcal{Q}(\dot{\mathbf{x}}_{\Lambda^{(k)}})$ in $\frac{1}{2}\left\|\mathcal{Q}(\dot{\mathbf{y}}) - \mathcal{P}(\dot{\mathbf{D}}_{\Lambda^{(k)}})\mathcal{Q}(\dot{\mathbf{x}}_{\Lambda^{(k)}})\right\|_2^2$ to $\mathbf{0}$, we obtain the minimizer $\mathcal{Q}(\dot{\mathbf{x}}^{(k)}_{\Lambda^{(k)}})$ and update $\dot{\mathbf{x}}^{(k)}_{\Lambda^{(k)}}$ as

$$\dot{\mathbf{x}}^{(k)}_{\Lambda^{(k)}} = \mathcal{Q}^{-1}\left(\left(\mathcal{P}\left(\dot{\mathbf{D}}_{\Lambda^{(k)}}\right)^T\mathcal{P}\left(\dot{\mathbf{D}}_{\Lambda^{(k)}}\right)\right)^{-1}\mathcal{P}\left(\dot{\mathbf{D}}_{\Lambda^{(k)}}\right)^T\mathcal{Q}(\dot{\mathbf{y}})\right). \tag{6}$$

Once we obtain the solution $\dot{\mathbf{x}}^{(k)}_{\Lambda^{(k)}}$ of the last iteration, then the optimal sparse $\dot{\mathbf{x}}^*$ satisfies $\dot{\mathbf{x}}^*_{\Lambda^{(k)}} = \dot{\mathbf{x}}^{(k)}_{\Lambda^{(k)}}$ and the other zeros.

4) Residual update: Refine residual as $\dot{\mathbf{r}}^{(k)} = \dot{\mathbf{y}} - \dot{\mathbf{D}}_{\Lambda^{(k)}}\dot{\mathbf{x}}^{(k)}_{\Lambda^{(k)}}$.

Typically, QOMP requires S iterations, whereas QGOMP only needs $\lceil S/s_0\rceil < S$ iterations, where $\lceil S/s_0\rceil$ is the ceiling operation. The steps of QGOMP are outlined in Algorithm 1.

3.2 Applications

The sparse representation by QGOMP can be applied for signal reconstruction, recognition, and clustering.

3.2.1 Color face recognition

As a typical multi-channel data, a color image can be represented as a quaternion vector $\dot{\mathbf{y}} = \mathbf{0} + \mathbf{y}_r\mathbf{i} + \mathbf{y}_g\mathbf{j} + \mathbf{y}_b\mathbf{k}$, where the RGB channels are integrated into a vector, respectively. The dictionary matrix $\dot{\mathbf{D}}$ is formed by stacking training samples as quaternion vectors in its columns.

Specifically, we consider a face recognition tasks [11] with N classes. Let C_i be the index set of class i samples and $C_1 \cup C_2 \cup \cdots \cup C_N = C$ is the index set covering all training samples. Given a test sample $\dot{\mathbf{y}}$, we obtain the sparse representation $\dot{\mathbf{x}}^*$ according to QGOMP. Then we calculate the residuals for each category by

$$r_i = \left\|\dot{\mathbf{y}} - \dot{\mathbf{D}}_{C_i}\dot{\mathbf{x}}^*_{C_i}\right\|_2^2, \quad i = 1, 2, \cdots, N. \tag{7}$$

Here, $\dot{\mathbf{x}}^*_{C_i}$ is the sub-vector of $\dot{\mathbf{x}}$, which aligned with the location in $\dot{\mathbf{D}}_{C_i}$. Finally, $\dot{\mathbf{y}}$ is identified in the class i with the smallest residual by $i = \min_{i=1,2,\cdots,N} r_i$.

Algorithm 1 QGOMP Algorithm

Input: $\dot{\mathbf{y}} \in \mathbb{H}^m$, $\dot{\mathbf{D}} \in \mathbb{H}^{m\times n}$, sparsity S, and the count of indices chosen per iteration s_0 ($s_0 \le S$ and $s_0 \le m/S$).
Initialization: iteration $k = 0$, $\Lambda^{(0)} = \emptyset$, $\dot{\mathbf{r}}^{(0)} = \dot{\mathbf{y}}$.
1: while $\|\dot{\mathbf{r}}^{(k)}\|_2^2 \ge 10^{-6}$ and $k < \lceil S/s_0\rceil$ do
2: $k = k + 1$.
3: Construct set $\boldsymbol{I}^{(k)}$ containing s_0 indices by Eq. (2).
4: Update the index set $\Lambda^{(k)} = \Lambda^{(k-1)} \cup \boldsymbol{I}^{(k)}$.
5: Update $\dot{\mathbf{x}}^{(k)}_{\Lambda^{(k)}}$ by Eq. (6).
6: Compute residual with $\dot{\mathbf{r}}^{(k)} = \dot{\mathbf{y}} - \dot{\mathbf{D}}_{\Lambda^{(k)}}\dot{\mathbf{x}}^{(k)}_{\Lambda^{(k)}}$.
7: end while
Output: The optimal $\dot{\mathbf{x}}^*$ with $\dot{\mathbf{x}}^*_{\Lambda^{(k)}} = \dot{\mathbf{x}}^{(k)}_{\Lambda^{(k)}}$ and the other zeros.

3.2.2 Color face clustering

The sparse representation by QGOMP can also be used in the clustering task. Ideally, samples in the same class should reside in the same subspace, and their sparse representations on the basis of this subspace can serve as the basis for clustering [12]. Specifically, for samples that need to clustering $\dot{\mathbf{D}} = [\dot{\mathbf{d}}_1, \dot{\mathbf{d}}_2, \cdots, \dot{\mathbf{d}}_n] \in \mathbb{H}^{m\times n}$ to be clustered, we first reprocess $\dot{\mathbf{D}}$ by applying an orthogonal projection transformation to obtain $\dot{\mathbf{D}}_{\text{pre}}$. Then we apply QGOMP to $\dot{\mathbf{d}}_i = \dot{\mathbf{D}}_{\text{pre}}\dot{\mathbf{x}}_i$ to solve for the optimal sparse coefficients $\dot{\mathbf{x}}^*_i$ for each sample $\dot{\mathbf{d}}_i$ in self-representation. Next, each representation $\dot{\mathbf{x}}^*_i$ is arranged in a quaternion matrix $\dot{\mathbf{X}}^*$. To effectively characterize the relationships between samples, we utilize $\dot{\mathbf{X}}^*$ to construct a real value affinity matrix $\hat{\mathbf{X}}$, which serves as the basis for the relationship graph of samples in clustering. The similarity between samples $\dot{\mathbf{d}}_i$ and $\dot{\mathbf{d}}_j$ ($i, j = 1, \ldots, n$) are defined as follows

$$\hat{\dot{x}}_{ij} = \hat{\dot{x}}_{ji} = \frac{1}{2}\left(\left|\dot{x}_{ij}\right| + \left|\dot{x}_{ji}\right|\right). \tag{8}$$

Here, $\hat{\dot{x}}_{ij}$ and $\dot{x}_{ij}$ are the (i, j)-th elements for $\hat{\mathbf{X}}$ and $\dot{\mathbf{X}}^*$, respectively. Subsequently, we employ the Normalized Cut

(NCut) algorithm [13] on $\hat{\mathbf{X}}$ to generate the final clustering results.

4 Experiments

This section demonstrates the experimental performance for QGOMP in the tasks of recovery, recognition and clustering to fully evaluate its effectiveness and efficiency.

4.1 Multi-channel sparse signal recovery

In this section, we show the signal recovery experiments including the two cases as 1D quaternion sparse signals and 2D color face images.

4.1.1 1D quaternion sparse signal recovery

We assess QGOMP's performance in recovering sparse signals from noisy measurements in the one dimensional case and analyze the parameter of indices chosen per iteration s_0. The comparative methods are classic QOMP and Qlasso algorithms. QGOMP$_{s_0}$ means to take s_0 indices per iteration in our method.

Experiments setting: We randomly generate a 600-dimensional quaternion sparse signal $\dot{\mathbf{x}}$ as the ground truth, where 5% ($S = 30$) elements are randomly drawn from the Gaussian distribution $\mathcal{N}(0, 1)$ while the remaining are set to zeros. The measurement is $\dot{\mathbf{y}} = \dot{\mathbf{D}}\dot{\mathbf{x}} + \dot{\mathbf{n}} \in \mathbb{H}^{100}$, where $\dot{\mathbf{n}}$ is noise following $\mathcal{N}(0, 1)$. The observed matrix $\dot{\mathbf{D}} = \mathbf{D}_0 + \mathbf{D}_1\mathbf{i} + \mathbf{D}_2\mathbf{j} + \mathbf{D}_3\mathbf{k} \in \mathbb{H}^{100\times 600}$ and each $\mathbf{D}_i$ is sampled from a standard normal distribution. The dvaluation metrics we used are running time and the relative reconstruction error RelErr as $\| \dot{\mathbf{x}} - \dot{\mathbf{x}}^* \|_2 / \| \dot{\mathbf{x}} \|_2$, where $\dot{\mathbf{x}}^*$ is the signal recovered by methods.

Recovery Results: Fig. 1 shows an example for the sparse signal recovery performance and their running times. We can find that the QGOMP$_3$ method outperforms Qlasso in recovering quaternion sparse signals and achieves comparable recovery performance to the QOMP method. Significantly, the running times for QGOMP$_3$ is half less than that of QOMP. This result validates the effectiveness of QGOMP$_3$ in selecting multiple most relevant atoms in a single iteration.

Parameter s_0 selecting: We examine the recovery performance for different s_0 values in QGOMP across signals with varying sparsity S from 5 to 40. Fig. 2 shows RelErr (left) and time (right) results. Here, we use the $s_0 = 2, 3, 10, 20$ and 40 and QOMP can be regarded as

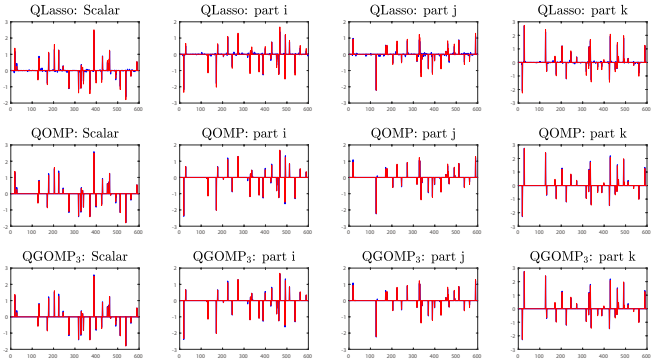

FIGURE 1. The recovery performances of comparative methods and QGOMP. The original simulated signal $\dot{\mathbf{x}}$ is marked in red, while the recovered signal $\dot{\mathbf{x}}^*$ is marked in blue. The RelErr/Time (s) are QLasso: 0.1525/14.0625; QOMP: 0.0578/1.125; QGOMP$_3$: 0.0578/0.375.

$s_0 = 1$. We can find that, QGOMP$_{40}$ exhibits a significant increase in reconstruction error due to incorrect atom selection when $s_0 > S$. The reconstruction error of QGOMP$_2$ and QGOMP$_3$ are comparable to that of the QOMP algorithm. But the running times for QOMP is the largest one among all of the methods. The QGOMP series demonstrate a significant advantage, with their runtime being notably shorter than that of QOMP. Hence, $s_0 = 2$ or 3 balances the recovery accuracy and time effectively, which is selected as the s_0 in the following experiments.

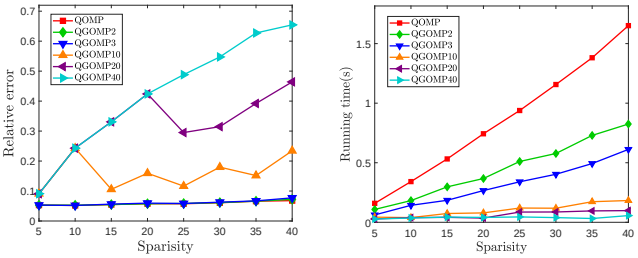

FIGURE 2. Sparse signals recovery results (average RelErr and Time(s) over 50 trials) for different sparsity levels and s_0 choices.

4.1.2 2D color face recovery

2D quaternion signals can effectively represent color images and are widely used in image processing. We use two datasets: AR and SCface [14, 15]. The AR contains 2600 images of 100 subjects (50 male, 50 female) with varying facial expressions, illumination, and natural occlusions by eyeglasses, scarves. We use images under different

FIGURE 3. Examples of AR (top) and SCface (bottom) datasets.

expressions and illumination conditions, totaling 1400 images for subsequent experiments. The SCface includes 130 subjects, each with 16 images, with low-resolution images captured under uncontrolled conditions. The SCface poses a significant challenge for color face tasks. Examples from AR and SCface are shown in Fig. 3.

Setting: All images in the AR are downsampled to size 83×60. The first four images of each subject in Session 1 serve as a dictionary $\dot{\mathbf{D}}$. The first image per subject in Session 2, 50% pixels with salt and pepper noise or 25% pixels with occlusion, is the test sample. The comparison methods are real-valued Lasso, OMP, GOMP, and QLasso, QOMP. We set $s_0 = 2$ in QGOMP and select PSNR as evaluation criteria.

Recovery from salt and pepper noise: In Fig. 4, the optimal results are bold. Under the influence of salt and pepper noise, real-valued methods fall short of the corresponding quaternion-valued methods in PSNR. QOMP and our QGOMP achieve optimal recovery results, particularly in preserving fine details like edges, textures, and smooth regions.

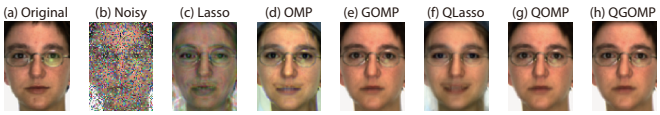

FIGURE 4. Recovery performances of 50% pixels damaged by salt and pepper noise. (a) Original image; (b) Noisy image; reconstructed images by various methods with PSNR: (c) Lasso: 18.28; (d) OMP: 19.93; (e) GOMP: 24.44; (f) QLasso: 22.19; (g) QOMP: **24.50**; (h) QGOMP: **24.50**.

Recovery from occlusion: In Fig. 5, the best results are bold. Real-valued methods struggle to distinguish occluded regions, leaving many baboon colors in the recovered images. In contrast, quaternion-based methods, leveraging their precise characterization of the relationships between color channels, successfully overcome this problem. Among these methods, QOMP and QGOMP yield the highest PSNR.

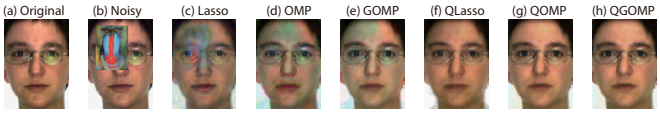

FIGURE 5. Recovery performances of 25% pixels covered by occlusion. (a) Original image; (b) Noisy image; reconstructed images by various methods with PSNR: (c) Lasso: 18.17; (d) OMP: 19.33; (e) GOMP: 22.20; (f) QLasso: 22.98; (g) QOMP: 25.22; (h) QGOMP: 25.22.

4.2 Color face recognition

In this section, we evaluate the capability of our QGOMP classifier in face recognition color. We analyze the recognition rate in the SCface dataset in varying proportions of training, which is one of the most challenges color face dataset since its low resolution. In this dateset, we use images for 40 subjects, with 16 images per person and each of them is resized to 20×15. We select images in different proportions for training and the remaining for testing. We show one trial of the experiment for the recognition in Tab. 1.

TABLE 1. Recognition rate (%) results of each method with different training percentage (p_t%) on the SCface dataset of 40 classes in one trial. The optimal results are bold, and suboptimal results are underlined.

p_t%	30	40	50	60	70
QLasso	79.5	79.5	82.2	**85.8**	82.5
QOMP	82.0	<u>83.8</u>	<u>85.0</u>	<u>85.4</u>	82.0
QGOMP_2	83.0	83.5	83.8	85.0	<u>85.5</u>
QGOMP_3	**85.0**	**84.8**	82.2	83.3	83.0
QGOMP_{10}	<u>84.3</u>	**84.8**	**86.3**	85.0	**87.0**

Result: In Tab. 1, we can find that across different training set sizes, QGOMP_{10} consistently shows the highest recognition rate in three experiments. This suggests that when the data is low resolution, selecting an appropriately large s_0 can better leverage the correlation among atoms of the same class.

4.3 Color face clustering

In this section, we conduct clustering performance on the AR dataset. In AR, each image is downsampled to a

TABLE 2. Clustering ACC (%) with different image sizes and the number of classes on AR dataset in one trial. The best results are in bold.

Classes	$C = 10$		$C = 50$		$C = 100$	
Size	8×6	20×15	8×6	20×15	8×6	20×15
K-means	29.3	31.0	21.9	22.7	19.8	20.2
LRR	35.9	38.9	13.0	14.8	6.9	9.1
TLRR	76.6	**100.0**	68.9	80.5	57.0	72.2
SSC	60.5	64.8	43.4	54.7	44.0	52.9
QLasso	92.9	70.7	73.2	74.3	**65.1**	66.2
QOMP	**98.6**	95.0	79.8	81.4	61.6	76.0
$QGOMP_3$	**98.6**	95.1	**81.7**	**82.9**	61.2	**76.1**

size of 20×15, and the first seven images of each subject from Session 1 and Session 2 are selected as the samples. We investigate the clustering performance for QGOMP varying different image size and the number of categories. The competing methods we used are K-means, Low-Rank Representation (LRR) [16], and Tensor Low-Rank Representation (TLRR) [17], Sparse Subspace Clustering (SSC) [18]. The parameters are recommended by the authors. The evaluation metric is clustering accuracy.

Result: In Tab. 2, we show one of the c lusting performance example. We can find that comparing to QOMP, QGOMP can achieve certain enhancements in clustering performance in most of the image sizes and categories, which demonstrates its strong adaptability to various tasks.

5 Conclusion

This paper proposes a Quaternion Generalized Orthogonal Matching Pursuit (QGOMP) algorithm in sparse representation for holistic processing of multi-channel signals. The algorithm leverages the correlations between atoms to more efficiently select s_0 atoms during each iteration, accelerating QOMP. In addition, we design classifiers and clustering algorithms based on QGOMP for recognition and clustering tasks. Both synthetic and real dataset experiment results exhibit the superiority and flexibility of QGOMP in quaternion sparse signal recovery, color image recovery, recognition and clustering.

Acknowledgments

This work was supported by the National Natural Science Foundation of China under Grant Nos. 62276111, 62076041 and 61806027. This work was supported by Research Grants of Huazhong Agricultural University of Grant No. 2662024XXPY005.

References

[1] Y. Pati, R. Rezaiifar, and P. Krishnaprasad, "Orthogonal matching pursuit: recursive function approximation with applications to wavelet decomposition," in Proceedings of 27th Asilomar Conference on Signals, Systems and Computers, pp. 40–44 vol.1, 1993.

[2] S. Miron, J. Flamant, N. L. Bihan, P. Chainais, and D. Brie, "Quaternions in signal and image processing: A comprehensive and objective overview," IEEE Signal Processing Magazine, vol. 40, no. 6, pp. 26–40, 2023.

[3] Y. Xu, L. Yu, H. Xu, H. Zhang, and T. Nguyen, "Vector sparse representation of color image using quaternion matrix analysis," IEEE Transactions on image processing, vol. 24, no. 4, pp. 1315–1329, 2015.

[4] Y. Dong, C. Zou, X. Xiao, and K. I. Kou, "Robust quaternion block orthogonal matching pursuit with its applications," Digital Signal Processing, vol. 158, p. 104946, 2025.

[5] D. Needell and R. Vershynin, "Signal recovery from incomplete and inaccurate measurements via regularized orthogonal matching pursuit," IEEE Journal of Selected Topics in Signal Processing, vol. 4, no. 2, pp. 310–316, 2010.

[6] J. Wang, S. Kwon, and B. Shim, "Generalized orthogonal matching pursuit," IEEE Transactions on Signal Processing, vol. 60, no. 12, pp. 6202–6216, 2012.

[7] W. R. Hamilton, Elements of quaternions. London: Longmans, Green, & Company, 1866.

[8] Y. Xu, L. Yu, H. Xu, H. Zhang, and T. Nguyen, "Vector sparse representation of color image using quaternion matrix analysis," IEEE Transactions on image processing, vol. 24, no. 4, pp. 1315–1329, 2015.

[9] J. Wang, S. Kwon, P. Li, and B. Shim, "Recovery of sparse signals via generalized orthogonal matching pursuit: A new analysis," IEEE Transactions on Signal Processing, vol. 64, no. 4, pp. 1076–1089, 2015.

[10] C. Zou, K. I. Kou, and Y. Wang, "Quaternion collaborative and sparse representation with application to color face recognition," IEEE Transactions on image processing, vol. 25, no. 7, pp. 3287–3302, 2016.

[11] W. A. Barrett, "A survey of face recognition algorithms and testing results," in Conference Record of the Thirty-First Asilomar Conference on Signals, Systems and Computers, vol. 1, pp. 301–305, IEEE, 1997.

[12] J. Oyelade, I. Isewon, O. Oladipupo, O. Emebo, Z. Omogbadegun, O. Aromolaran, E. Uwoghiren, D. Olaniyan, and O. Olawole, "Data clustering: Algorithms and its applications," in 2019 19th international conference on computational science and its applications (ICCSA), pp. 71–81, IEEE, 2019.

[13] C. Wang, X. Chen, F. Nie, and J. Z. Huang, "Directly solving normalized cut for multi-view data," Pattern Recognition, vol. 130, p. 108809, 2022.

[14] J. Flamant, S. Miron, and D. Brie, "A general framework for constrained convex quaternion optimization," IEEE Transactions on Signal Processing, vol. 70, pp. 254–267, 2021.

[15] M. Grgic, K. Delac, and S. Grgic, "Scface–surveillance cameras face database," Multimedia tools and applications, vol. 51, pp. 863–879, 2011.

[16] G. Liu, Z. Lin, and Y. Yu, "Robust subspace segmentation by low-rank representation," in Proceedings of the 27th international conference on machine learning (ICML-10), pp. 663–670, 2010.

[17] P. Zhou, C. Lu, J. Feng, Z. Lin, and S. Yan, "Tensor low-rank representation for data recovery and clustering," IEEE transactions on pattern analysis and machine intelligence, vol. 43, no. 5, pp. 1718–1732, 2019.

[18] E. Elhamifar and R. Vidal, "Sparse subspace clustering: Algorithm, theory, and applications," IEEE Transactions on Pattern Analysis and Machine Intelligence, vol. 35, no. 11, pp. 2765–2781, 2013.